Dihydrogen with Frequency of Motion Near the ^{1}H Larmor Frequency. Solid-State Structures and Solution NMR Spectroscopy of Osmium Complexes *trans*-$[Os(H{\cdot\cdot}H)X(PPh_2CH_2CH_2PPh_2)_2]^+$ (X = Cl, Br)

Patricia A. Maltby,† Marcel Schlaf,† Martin Steinbeck,† Alan J. Lough,† Robert H. Morris,*,† Wim T. Klooster,‡ Thomas F. Koetzle,‡ and Ramesh C. Srivastava‡,§

Contribution from the Departments of Chemistry, University of Toronto, 80 St. George Street, Toronto, Ontario M5S 3H6, Canada, and Brookhaven National Laboratory, Upton, New York 11973

Received August 23, 1995. Revised Manuscript Received February 5, 1996⊗

Abstract: A high-yield route to the new complexes $OsBr_2(dppe)_2$ and *trans*-$OsHBr(dppe)_2$ starting from $(NH_4)_2[OsBr_6]$ is described. The new 5-coordinate complexes $[OsX(dppe)_2]PF_6$ (X = Cl (**8Os**) and X = Br (**9Os**)) are prepared by reaction of *cis*-$OsX_2(dppe)_2$ with $NaPF_6$. Complexes **8Os** and **9Os** consist of distorted trigonal bipyramidal cations with "Y"-shaped equatorial planes. They react in CH_2Cl_2 with H_2 or HD (1 atm) to give complexes *trans*-$[Os(H{\cdot\cdot}H)X(dppe)_2]PF_6$ (X = Cl (**1Os**PF_6), X = Br (**2Os**PF_6)) or *trans*-$[Os(H{\cdot\cdot}D)X(dppe)_2]PF_6$, respectively. The last complexes have J(H,D) = 13.9 and 13.7 Hz, respectively. The BF_4^- salts of these complexes, **1Os**BF_4 and **2Os**BF_4, respectively, are prepared by reacting *trans*-$OsHX(dppe)_2$ with $HBF_4{\cdot}Et_2O$ or $DBF_4{\cdot}Et_2O$. These complexes are characterized by NMR, IR, and FAB MS. The single-crystal X-ray and neutron diffraction studies of **1Os**PF_6 revealed an elongated H··H ligand with d_{HH} = 1.11(6) (X-ray) or 1.22(3) Å (neutron) occupying one site in an octahedral complex. The X-ray diffraction study of **2Os**BF_4 produced a similar structure with d_{HH} = 1.13(8) Å. One fluorine of the anion in each structure is positioned near the acidic H_2 ligand. A linear relationship between d_{HH} and J(H,D) for many dihydrogen complexes is used to indicate that complexes **1Os** and **2Os** have H−H distances of about 1.2 Å in solution. Plots of ln(T_1) versus inverse temperature for **1Os** and **2Os** are distorted from the usual "V" shape, suggesting that the rotational frequency of the H_2 ligand is near that of the Larmor frequency. Therefore the d_{HH} for **1Os** is between the values of 1.04 and 1.31 Å calculated from the T_1(min) for fast and slow spinning H_2, respectively. The chloride ligand in *trans*-$[Os(H{\cdot\cdot}H)Cl(L)_2]^+$ buffers the effect of changing the cis ligands L from dppe to depe to dcpe so that there is little change in the H−H distance. Complexes **1Os** and **2Os** have pK_a values of 7.4 and 5.4, respectively, while *trans*-$[Os(H_2)H(dppe)_2]^+$ is much less acidic with a pK_a of 13.6. These pK_a values and some $E_{1/2}$ values are used to show that **1Os** and **2Os** are dihydride-like even though they have relatively short H−H distances. Properties of *trans*-$[Os(H{\cdot\cdot}H)Cl(depe)_2]BF_4$ (**3Os**) are also reported.

Introduction

Recently we studied the differences in the trans influence of chloride compared to hydride on the properties of the dihydrogen ligand in the complexes *trans*-$[Ru(H_2)XL_2]^+$ (X = Cl, L = dppe[1] (**1Ru**), depe (**3Ru**); X = H, L = dppe (**5Ru**), depe (**6Ru**)).[2] Although the T_1 and J(H,D) NMR data clearly indicated that the dihydrogen ligand was elongated in the chloride complex **1Ru** relative to the hydride complex, **5Ru**, the H−H bond length in the former complex could not be unambiguously established in solution by NMR methods or in the solid-state for **1Ru**PF_6 by single-crystal X-ray analysis. However complex **1Ru** has a much lower pK_a value of 6 compared to the value of 15 for **5Ru**; this was related to a smaller H−H bond energy in **1Ru** compared to the one in **5Ru**. Here we establish the H−H distances in the solid-state and in solution for the corresponding osmium(II) complexes *trans*-$[Os(H{\cdot\cdot}H)XL_2]^+$ (L = dppe, X = Cl (**1Os**), X = Br (**2Os**), L = depe, X = Cl (**3Os**)). During the course of this work Mezzetti et al.[3] prepared and characterized in solution the related complexes *trans*-$[Os(H{\cdot\cdot}H)Cl(dcpe)_2]BPh_4$ (**4Os**) and the osmium(IV) trihydride complex $[OsH_3(dcpe)_2]BPh_4$ (**7Os**).[1] Also the single-crystal neutron diffraction study of *trans*-$[Os(H{\cdot\cdot}H)(OAc)(en)_2]PF_6$ was reported.[4] These complexes provide useful comparisons to those of the present work.

Determining the H−H distance in solution by use of the T_1(min) method is complicated by the motion of the dihydrogen ligand. Dihydrogen ligands with rotational frequencies much greater than the proton Larmor frequency ($2\pi\nu$, where ν is the NMR spectrometer frequency) have dipolar relaxation rates which are four times slower than ligands with the same H−H distances but with rotational frequencies much less than $2\pi\nu$. It is already established by use of T_1(min) and J(H,D) values that the complex *trans*-$[Os(H_2)H(dppe)_2]BF_4$ (**5Os**) in solution

† University of Toronto.
‡ Brookhaven National Laboratory.
§ Permanent address: Department of Physics, Indian Institute of Technology, Kanpur 208016, India.
⊗ Abstract published in *Advance ACS Abstracts,* May 15, 1996.

(1) Ligand abbreviations: $PR_2CH_2CH_2PR_2$, R = phenyl (dppe), ethyl (depe), cyclohexyl (dcpe). Complex numbering: the anion is indicated (e.g., **1Os**PF_6) when solid-state properties are discussed. We have no evidence that solution properties are influenced by the anion. However the solution NMR properties refer to **1Os**PF_6, **2Os**PF_6, and **3Os**BF_4 unless specified otherwise.

(2) Chin, B.; Lough, A. J.; Morris, R. H.; Schweitzer, C. T.; D'Agostino, C. *Inorg. Chem.* **1994**, *33,* 6278−6288.

(3) Mezzetti, A.; Del Zotto, A.; Rigo, P.; Farnetti, E. *J. Chem. Soc., Dalton Trans.* **1991**, 1525−1530.

(4) Hasegawa, T.; Li, Z.; Parkin, S.; Hope, H.; McMullan, R. K.; Koetzle, T. F.; Taube, H. *J. Am. Chem. Soc.* **1994**, *116,* 4352−4356.

S0002-7863(95)02904-0 CCC: $12.00

has a rapidly spinning dihydrogen ligand with an H−H distance of 0.99 ± 0.01 Å.[5] It has an H−H distance of 0.99 Å according to a solid-state NMR study.[6] The complexes *trans*-[Os(H··H)(OAc)(en)$_2$]PF$_6$ and [Ru(C$_5$Me$_5$)(H··H)(dppm)]BF$_4$ are established to have H$_2$ ligands with slow rotation rates (rate $\ll \nu$).[7] Recently Jalon et al. have shown that [Nb(C$_5$H$_4$SiMe$_3$)$_2$(HD)(PMe$_2$Ph)]$^+$ has a slowly rotating, elongated H··D ligand.[8] For the complex *trans*-[Os(H··H)H(depe)$_2$]$^+$ (**6Os**),[9,10] which contains the depe ligand which is more electron-donating than dppe, a rapid equilibrium has been proposed such that the observed NMR properties are the weighted average of the those of the dihydrogen hydride, [Os(H$_2$)H(L)$_2$]$^+$, and trihydride ([OsH$_3$(L)$_2$]$^+$) forms.[5] Such a proposition was required to explain the solvent-dependent T_1(min) values and the solvent- and temperature-dependent J(H,D) coupling of [Os(H··D)D(depe)$_2$]$^+$. In a communication of the present work, the complex **3Os** was also proposed to have such a rapid equilibrium.[11] Here we provide the first evidence for complexes of a dihydrogen ligand that have a frequency of motion near the ^{1}H Larmor resonance frequency.

Experimental Section

All operations were conducted under a purified nitrogen or argon atmosphere using vacuum line and glovebox techniques. All solvents were dried over appropriate reagents and distilled under N$_2$ before use. Deuterated solvents were dried over Linde-type 4 Å molecular sieves and degassed with several evacuate/refill cycles prior to use. Reagent-grade chemicals were used as purchased from Aldrich Chemical Co., Inc., unless otherwise stated. Phosphine ligands were purchased from Strem Chemical Co. or Digital Speciality Chemicals Ltd. The complexes (NH$_4$)$_2$[OsBr$_6$],[12] *cis*-OsCl$_2$(dppe)$_2$,[13] *trans*-[Os(H$_2$)H(dppe)$_2$]BF$_4$ (**5Os**),[5,14] and OsH$_2$(dppe)$_2$,[5,14] were prepared as described previously.

Microanalytical results and FAB MS (NBA matrix), IR, and ^{1}H and ^{31}P NMR spectra were obtained as previously described.[2] ^{31}P NMR were proton decoupled, except for one experiment involving *trans*-[Os(H··D)Cl(dppe)$_2$]BF$_4$. ^{1}H NMR spectra were simulated by use of the FIRSTORDER simulation program written by T. Burrow. T_1 measurements were made at 500, 400, and 300 MHz using the inversion−recovery method. The concentration of the sample must be the same for a comparison to be made of results obtained at different magnetic fields; therefore, the sample was sealed in a 5 mm NMR tube for the measurements. Pulses were calibrated to exactly 90° and 180° at all reported temperatures. The temperatures were calibrated by use of the methanol method.

Preparation of *cis*-OsBr$_2$(dppe)$_2$. (NH$_4$)$_2$[OsBr$_6$] (0.267 g, 0.378 mmol), dppe (0.608 g, 1.53 mmol), 70 mL of EtOH, and 60 mL of MeOH were added to a 250 mL two-neck round-bottom flask. A condenser was attached, and the dark slurry was purged by use of several vacuum/Ar cycles. The mixture was refluxed under Ar for 33 h; a pale-yellow solid in a yellow liquor was observed. The volume was reduced to 100 mL, and the pale-yellow solid was filtered from the solution. The solid was washed with MeOH (10 mL) and dried *in vacuo*. *cis*-OsBr$_2$(dppe)$_2$ (0.410 g) was obtained (92% yield). This crude material is pure enough for subsequent reactions. However it can be recrystallized in a dinitrogen atmosphere. *cis*-OsBr$_2$(dppe)$_2$ (0.044 g), acetone (7 mL), and benzene (3 mL) were heated, and the warm solution was filtered through a Kimwipe tissue suspended in a Pasteur pipette. The volume was reduced by one-half and the pale yellow solution transferred to a vial. An equal volume of hexanes was carefully added, and diffusion was allowed to occur overnight. The pale-yellow microcrystalline solid was filtered from the pale-yellow liquor and dried *in vacuo*. Anal. Calcd for C$_{52}$H$_{48}$OsP$_4$Br$_2$: C, 54.46; H, 4.22. Found: C, 54.57; H, 4.30. FAB MS: calcd for C$_{52}$H$_{48}$^{192}OsP$_4$^{79}Br$_2$ 1146.1. FAB MS obsd (2-nitrophenyl octyl ether matrix): 1146.5 (M$^+$), 1067.5 (M$^+$ − Br), 987.6 (M$^+$ − H,2Br), 985.7 (M$^+$ − 3H,2Br). NMR δ(^{31}P, CH$_2$Cl$_2$): 1.2 (t, ^2J(P,P) 5.4), −1.3 (t).

Preparation of [OsCl(dppe)$_2$]PF$_6$ (8Os). *cis*-OsCl$_2$(dppe)$_2$ (300 mg, 0.27 mmol) and NaPF$_6$ (100 mg, 0.8 mmol) were dissolved in a mixture of 15 mL of THF and 15 mL of CH$_2$Cl$_2$. The reaction was stirred at room temperature for 48 h to give a dark-brown solution. The reaction mixture was evaporated to dryness and redissolved in 15 mL of CH$_2$Cl$_2$. The dark-brown solution was filtered through Celite/cotton wool to remove the excess NaPF$_6$ and the NaCl formed in the reaction. This reaction solution can be used to prepare **1Os** as described below. Dark-red crystals of **8Os** suitable for X-ray diffraction analysis[15] were obtained within 5 d by slow diffusion of diethyl ether into a CH$_2$Cl$_2$ solution of **8Os** at room temperature. NMR δ(^{31}P, 121.5 MHz, CH$_2$Cl$_2$): 48.4 (s), 26.0 (s), −143 ppm (^1J(P,F) 700 Hz).

Preparation of [OsBr(dppe)$_2$]PF$_6$ (9Os). This was prepared from *cis*-OsBr$_2$(dppe)$_2$ by the same method used for **8Os**. NMR δ(^{31}P, CH$_2$Cl$_2$): 51.1 (br), 23.5 (br), −143 ppm (^1J(P,F) 700 Hz). The reaction solution was used to prepare **2Os**PF$_6$ as described below.

Preparation of *trans*-OsHCl(dppe)$_2$ (10Os). *trans*-[OsHCl(dppe)$_2$]·C$_6$H$_6$ was first prepared by Chatt and Hayter in 40% yield by the reaction of *cis*-OsCl$_2$(dppe)$_2$ and excess LiAlH$_4$. The ν(OsH) mode was reported at 2046 cm^{-1}.[16] We obtained a mixture of OsH$_2$(dppe)$_2$ and *trans*-OsHCl(dppe)$_2$ by following their method. The hydridochloro complex was prepared from **5Os** by the displacement of dihydrogen by chloride as described below.

Complex **5Os** (0.105 g, 0.092 mmol) was dissolved in acetone (10 mL), and then LiCl (0.025 g, 0.60 mmol) was added under N$_2$. The mixture was stirred, and after 45 min, a pale-yellow precipitate had formed. After 3 h a ^{31}P NMR spectrum of the reaction liquor indicated that no **5Os** remained in solution and the reaction was therefore complete. The acetone was removed under vacuum, and the benzene-soluble portion was isolated by filtration through Celite. The benzene was removed under vacuum. Acetone (5 mL) was added, and the mixture was cooled. The pale-yellow solid was collected by filtration and dried under vacuum (0.070 g, 74%). Anal. Calcd for C$_{52}$H$_{49}$ClOsP$_4$: C, 61.02; H, 4.83. Found: C, 60.59; H, 4.74. FAB MS: calcd for C$_{52}$H$_{49}$^{35}Cl^{192}OsP$_4$ 1024, observed 1025 (MH$^+$ = **1Os**) and 987.7 (M$^+$ − H,Cl). NMR δ(^{1}H, C$_6$D$_6$, 200 MHz): 7.6−6.8 (m, 40 H, Ph), 2.57 (m, 4 H, CH$_2$), 2.00 (m, 4 H, CH$_2$), −20.40 (qnt, 1H, ^2J(H,P) = 15.4 Hz, OsH). NMR δ(^{31}P, C$_6$D$_6$): 30.5 (s). IR (Nujol): 2124 cm^{-1} (w, ν(OsH)).

Preparation of *trans*-OsHBr(dppe)$_2$ (11Os). The following sequence of chemicals was added to a 1 L two-neck round-bottom flask: (NH$_4$)$_2$[OsBr$_6$] (1.21 g, 1.72 mmol), dppe (1.50 g, 3.76 mmol), 250 mL of EtOH, and 250 mL of MeOH. A glass stopper and a condenser fitted with a gas inlet were attached, and the gray slurry was degassed using several vacuum and argon refill cycles. The reaction mixture was refluxed for 19 h under Ar, and a pale-yellow solid in a yellow liquor was formed. The mixture was allowed to cool and the solvent volume reduced by one-half. The solid was filtered, washed with MeOH (15 mL), and dried *in vacuo*; 1.007 g (55% yield) of *trans*-OsHBr(dppe)$_2$ was obtained. FAB MS: calcd for C$_{52}$H$_{49}$^{192}OsP$_4$^{79}Br 1068, obsd 1069 (MH$^+$ = **2Os**), 988 (overlapping 988 (M$^+$ − H, Br) and 990 (MH$^+$ − Br) envelopes). IR(Nujol): 2174 (w, ν(OsH)), 1952, 1988, 1811, 1732 cm^{-1} (br, vw, δ(CH) overtones). NMR δ(^{31}P, CH$_2$Cl$_2$): 28.7 (s). NMR δ(^{1}H, CD$_2$Cl$_2$): 7.35−6.95 (m, 40H, Ph), 2.66 (m, 4H, CH$_2$), 2.10 (m, 4H, CH$_2$), −20.38 (qnt, 1H, J(H,P) = 15.3 Hz, OsH).

(5) Earl, K. A.; Jia, G.; Maltby, P. A.; Morris, R. H. *J. Am. Chem. Soc.* **1991**, *113*, 3027−3039.
(6) Wisniewski, L. L.; Zilm, K. W. Private communication.
(7) Klooster, W. T.; Koetzle, T. F.; Jia, G.; Fong, T. P.; Morris, R. H.; Albinati, A. *J. Am. Chem. Soc.* **1994**, *116*, 7677−7681.
(8) Jalon, F. A.; Otero, A.; Manzano, B. R.; Villasenor, E.; Chaudret, B. *J. Am. Chem. Soc.* **1995**, *117*, 10123−10124.
(9) The H··H or H··D notation signifies the probable presence of an elongated (>1.0 Å) H$_2$ or HD ligand with J(H,D) < 25 Hz. See ref 10.
(10) Jessop, P. G.; Morris, R. H. *Coord. Chem. Rev.* **1992**, *121*, 155−284.
(11) Cappellani, E. P.; Maltby, P. A.; Morris, R. H.; Schweitzer, C. T.; Steele, M. R. *Inorg. Chem.* **1989**, *28*, 4437−4438.
(12) Dwyer, F. P.; Hogarth, J. W. *Inorg. Synth.* **1957**, *5*, 204.
(13) Chatt, J.; Hayter, R. G. *J. Chem. Soc.* **1961**, 896−904.
(14) Cappellani, E. P.; Drouin, S. D.; Jia, G.; Maltby, P. A.; Morris, R. H.; Petroff, A.; Schweitzer, C. T.; Xu, W. Manuscript in preparation.
(15) Lough, A. J.; Morris, R. H.; Schlaf, M. *Acta Crystallogr., Sect. C*, in press.
(16) Chatt, J.; Hayter, R. G. *J. Chem. Soc.* **1961**, 2605−2611.

Preparation of *trans*-OsHCl(depe)$_2$ (12Os). The complex was prepared using a modified version of Chatt and Hayter's method; NMR data were not given when this complex was first described.[13] A slurry of $LiAlH_4$ (0.073 g, 1.9 mmol) in *ca.* 10 mL of THF was added to a stirred pale-yellow solution of *cis*-OsCl$_2$(depe)$_2$ (0.400 g, 0.59 mmol) in 15 mL of THF. The gray slurry was refluxed for 25 min and allowed to cool. Excess $LiAlH_4$ was neutralized by the controlled addition of 7 mL of ethanol (dihydrogen gas is evolved at this step). After solvent evaporation, the gray residue was treated with a total of 45 mL of THF and the bulk of the lithium salts were removed by filtration through THF-saturated Celite. The pale-yellow filtrate volume was reduced to dryness, NaCl (0.049 g, 0.84 mmol) and acetone (30 mL) were added, and the milky mixture was refluxed for 2.5 h. The *trans*-OsHCl(depe)$_2$ product was isolated in the following manner. Acetone was removed under vacuum, and the portion soluble in benzene (45 mL in total) was filtered through benzene-saturated Celite. The pale yellow filtrate volume was reduced to dryness and a minimal volume of acetone ($\leq$5 mL) added. The yellow solution was cooled for 1 day, and the resulting white needles were removed from the yellow liquor. A total of 0.185 g (47% yield) were obtained. NMR δ(^{1}H, benzene-d_6): $-$22.8 (qnt, J(H,P) = 15.3 Hz). NMR δ(^{31}P, acetone): 33.4 (s). IR (Nujol): 2050 cm^{-1} (m, ν(OsH)).

Preparation of *trans*-[Os(H··H)Cl(dppe)$_2$]BF$_4$ (1OsBF$_4$). *trans*-OsHCl(dppe)$_2$, (**10Os**) (0.060 g, 0.059 mmol) was suspended in 15 mL of diethyl ether under 1 atm of dinitrogen. HBF$_4$·Et$_2$O ($\sim$7 μL, excess) was added dropwise with stirring. The mixture was stirred for 10 min and then cooled. The liquor was removed from the cream-colored solid by decantation and replaced with fresh diethyl ether (15$-$20 mL). The slurry was stirred and allowed to cool, and the solvent containing any excess HBF$_4$·Et$_2$O was removed by decantation. The washing cycle was repeated several times, and the product was then filtered and dried under vacuum (0.060 g, 92%). The compound is soluble in CH$_2$Cl$_2$ but has a low solubility in THF or acetone. FAB MS: calcd for $C_{52}H_{50}{}^{35}Cl^{192}OsP_4$ 1025.2, obsd 1025.3 (M$^+$), 1023.3 (M$^+$ $-$ 2H), 989.3 (M$^+$ $-$ H,Cl), and 987.3 (M$^+$ $-$3H,Cl). NMR δ(^{1}H, CD$_2$Cl$_2$, 400 MHz): 7.4$-$6.9 (m, 40 H, Ph), 2.83 (m, 4 H, CH$_2$), 2.23 (m, 4 H, CH$_2$), $-$11.45 (qnt, 2H, ^2J(H, P) = 11.6 Hz, OsH$_2$). NMR δ(^{31}P, CH$_2$Cl$_2$, 121.47 MHz): 20.8 (s). NMR δ(^{31}P, THF, 121.47 MHz): 23.1 (s). T_1 data are provided in Table 3 (see below). The NMR data previously reported[11] for the complex *trans*-[Os(H··H)Cl(dppe)$_2$]BF$_4$ are in error. NMR signals emanating from the complex *trans*-[Os(CH$_3$CN)H(dppe)$_2$]$^+$, formed from **5Os** and acetonitrile present in the solvents as a contaminant, were erroneously assigned to the *trans*-[Os(H··H)Cl(dppe)$_2$]$^+$ complex.

Clear colorless crystals of **1Os**BF$_4$ suitable for X-ray analysis were obtained by slow vapor diffusion of diethyl ether into a CH$_2$Cl$_2$ solution of the complex over a 14 h period under N$_2$. Details of this structure, which was not completely solved because of disorder problems, can be found elsewhere.[17] The monoclinic cell dimensions at 173 K were found to be a = 15.808(2) Å, b = 16.967(3) Å, c = 17.614(4) Å, and β = 102.44(1)° in the space group $P2_1/n$ with Z = 4, formula wt 1111.32, and V = 4613.4(15) Å^3.

Preparation of *trans*-[Os(H··H)Cl(dppe)$_2$]PF$_6$ (1OsPF$_6$). Dihydrogen gas was bubbled through a dark-brown solution of **8Os** in CH$_2$Cl$_2$. Within 2 min, the solution cleared and the color changed to a light green. The solution was layered with an equal volume of diethyl ether. Within 1 week at room temperature X-ray-grade light-green crystals formed coincident with decolorization of the mother liquor. Overall yield starting from *cis*-OsCl$_2$(dppe)$_2$ to **8Os** and then **1Os**PF$_6$ was 85%. The structure was determined by single-crystal X-ray and neutron diffraction studies (see below). The NMR data are identical to those of **1**BF$_4$ (see above) apart from the ^{31}P resonance of the PF$_6^-$ anion which appears as a septet at $-$143 ppm, ^1J(P,F) 700 Hz.

Observation of *trans*-[Os(H··D)Cl(dppe)$_2$]$^+$ (1Os-d_1). Method 1. *trans*-OsHCl(dppe)$_2$ (**10Os**) (0.035 g, 0.034 mmol) was suspended, under 1 atm of argon, in 13 mL of diethyl ether containing 0.07 mL of D$_2$O. Approximately 120 μL of HBF$_4$·Et$_2$O was then added to produce DBF$_4$ *in situ*. The mixture was stirred for 25 min. After 5 min the suspension color had turned from pale yellow to white. The liquor was removed, and the solid was washed with diethyl ether by two agitation/decantation cycles and then dried under vacuum. This was dissolved in CD$_2$Cl$_2$ or acetone-d_6. Method 2. Complex **8Os** in CD$_2$Cl$_2$ was reacted with HD gas (generated from NaH and D$_2$O); this gave a purer solution than method 1. NMR δ(^{1}H, CD$_2$Cl$_2$, 500 MHz): $-$11.58 (1:1:1 t of qnt, 1H, J(H,D) = 13.9 $\pm$ 0.2, J(H,P) = 11.7, Os(H··D)). NMR δ(^{31}P, CD$_2$Cl$_2$): 20.9 (s).

Preparation of *trans*-[Os(H··H)Br(dppe)$_2$]BF$_4$ (2OsBF$_4$). *trans*-OsHBr(dppe)$_2$ (0.393 g, 0.359 mmol) was partially dissolved in 5 mL of CH$_2$Cl$_2$. Approximately 90 μL of HBF$_4$·Et$_2$O was added in portions over a 2$-$3 min period with stirring. The pale-yellow suspension turned dark brown at first but then became pale brown within 10 min. The solution was layered with diethyl ether, and the precipitation of large, clear, pale-brown crystals started immediately. Yield: $\approx$80%. NMR δ(^{1}H, CD$_2$Cl$_2$, 400 MHz): $-$11.45 (br qnt, ^2J(H, P) = 11.5 Hz, OsH$_2$). NMR δ(^{31}P, CH$_2$Cl$_2$, 121.47 MHz): 17.6 (s).

Preparation of *trans*-[Os(H··H)Br(dppe)$_2$]PF$_6$ (2OsPF$_6$). This complex was prepared by starting from **9Os** in a fashion similar to the preparation of **1Os**PF$_6$. NMR δ(^{1}H, CD$_2$Cl$_2$, 400 MHz): $-$11.46 (qnt, ^2J(H,P) = 11.9 Hz, OsH$_2$). NMR δ(^{31}P, CH$_2$Cl$_2$, 121.47 MHz): 17.6 (s), $-$143 ppm (^1J(P,F) 700 Hz). T_1 data are provided in Table 3.

Observation of *trans*-[Os(H··D)Br(dppe)$_2$]$^+$ (2Os-d_1). Complex **9Os** in CD$_2$Cl$_2$ was reacted with HD gas as above. NMR δ(^{1}H, CD$_2$Cl$_2$, 293 K, 400 MHz): $-$11.6 (1:1:1 t of qnt, ^2J(H,P) 11.9 Hz, ^1J(H,D) 13.75).

Preparation of *trans*-[Os(H··H)Cl(depe)$_2$]BF$_4$ (3Os). *trans*-OsHCl(depe)$_2$ (0.100 g, 0.156 mmol) was partially dissolved in 7 mL of diethyl ether. Under 1 atm of dinitrogen a diluted HBF$_4$·Et$_2$O solution was added dropwise with stirring until a white precipitate formed. The mixture was cooled and the liquor removed by decantation. Fresh diethyl ether was added, and the decantation process was repeated. The white solid was filtered from cold diethyl ether and dried *in vacuo* (0.074 g, 65% yield). The product was crystallized from acetone by diffusion of diethyl ether vapor. Anal. Calcd for $C_{20}H_{50}BF_4ClOsP_4$: C, 33.05; H, 6.93. Found: C, 32.98; H, 7.00. NMR δ(^{1}H, acetone-d_6, 400 MHz): 2.45 (m, 4 H, PCH$_2$CH$_2$P), 2.31 (m, 4 H, PCH$_2$CH$_2$P), 2.0$-$1.75 (m, 16 H, CH$_2$), 1.18 (m, 12H, CH$_3$), 1.09 (m, 12H, CH$_3$), $-$13.81 (qnt, 2H, ^2J(H,P) = 11.7 Hz, OsH$_2$). NMR δ(^{31}P, acetone, 81 MHz): 25.8 (s). IR (Nujol): 1050 cm^{-1} (s, BF$_4^-$).

Acetone solutions of **3Os** turn a wine-red color after several days at room temperature; broad resonances are observed in the ^{1}H NMR spectrum: δ(^{1}H, acetone-d_6, 200 MHz) 8.3, 6.4, 2.7, $-$0.7, $-$4.3, $-$10.4, $-$24.6.

pK_a Determination of 1Os. A sample of the complex (26 mg, 0.02 mmol) was dissolved in 4 mL of CH$_2$Cl$_2$. The ^{31}P NMR spectrum was a single peak at 20.75. An aliquot solution of PPhMe$_2$ (30 mg) in CH$_2$Cl$_2$ (10 mL) was prepared. One equivalent (1 mL, 0.02 mmol of PPhMe$_2$) of this solution was added to the solution of the complex and the ^{31}P NMR acquired immediately using a gated decoupling ^{31}P{^{1}H} routine with delay times of 10 s between pulses. An NMR spectrum recorded 1 h later did not show any change in spectral appearance and relative integral values. A second equivalent of the phosphine solution was added and the ^{31}P NMR recorded with the relative integral values showing a clear shift of the equilibrium toward protonated phosphine HPPhMe$_2^+$. Over time some *trans*-[Os(PPhMe$_2$)Cl(dppe)$_2$]PF$_6$ is formed by substitution of the H··H with free phosphine. This reaction is slow and does not influence the acid$-$base equilibrium. Observed NMR shifts: PPhMe$_2$, $-$46.08 (s); [HPPhMe$_2$]$^+$, $-$0.35 (d, J(H,P) = 515.2 Hz); *trans*-[Os(H··H)Cl(dppe)$_2$]PF$_6$, +20.75 (s); *trans*-OsHCl(dppe)$_2$, 30.41 (s); *trans*-[Os(*PPhMe$_2$*)Cl(dppe)$_2$]PF$_6$, $-$63.35 (s); *trans*-[Os(PPhMe$_2$)Cl(*dppe*)$_2$][PF$_6$], 22.45 (s). For PPhMe$_2$ and [HPPhMe$_2$]$^+$ the reported shifts represent extreme values for complete deprotonation/protonation. In the presence of both the protonated and unprotonated form the peaks coalesce to a single broad signal. The observed shift is the weighted average of the two extreme values, i.e. ppm(obsd) = x ppm(PPhMe$_2$) + y ppm([HPPhMe$_2$]$^+$) with x and y as the relative concentrations.

pK_a Determination of 2Os. **11Os** (50 mg, 0.047 mmol) and P(p-CH$_3$OC$_6$H$_4$)$_3$ (15 mg, 0.04 mmol) are dissolved in 5 mL of CH$_2$Cl$_2$. An 85% solution of HBF$_4$·Et$_2$O (8 μL, 0.05 mmol) in Et$_2$O was added and the ^{31}P NMR spectrum acquired immediately using a gated decoupling ^{31}P{^{1}H} routine with delay times of 10 s between pulses.

(17) Maltby, P. A. Ph.D. Thesis, University of Toronto, 1993.

Table 1. Crystal Data, Details of Intensity Measurements, and Structure Refinements for *trans*-[Os(H··H)X($PPh_2CH_2CH_2PPh_2$)$_2$]Y (X = Cl, Y = PF_6 (**1Os**) and X = Br, Y = BF_4 (**2Os**))

	X-ray, **1Os**	neutron, **1Os**	X-ray, **2Os**
empirical formula	$C_{52}H_{50}ClF_6OsP_5$	$C_{52}H_{50}ClF_6OsP_5$	$C_{52}H_{50}BrOsP_4BF_4$
fw	1169.4	1169.4	1155.7
crystal system	monoclinic	monoclinic	monoclinic
space group	$P2_1/c$	$P2_1/c$	$P2_1/n$
cell dimensions			
a, Å	15.054(3)	15.142(8)	15.690(2)
b, Å	17.295(3)	17.283(5)	17.259(4)
c, Å	18.481(4)	18.47(3)	17.508(2)
β, deg	101.37(3)	101.5(1)	102.51(2)
V, Å^3	4717(1)	4736(5)	4629(1)
T, K	110	20.0(5)	150
Z	4	4	4
d_{calcd}, g cm^{-3}	1.647	1.640	1.658
μ, cm^{-1}	29.9	1.896	38.1
radiation	Mo K$\bar{\alpha}$	neutrons, λ = 1.163 95(10) Å	Mo K$\bar{\alpha}$
2θ range, deg	2.0−54.0	5.0−108.0	4.0−54.0
scan type	ω:2θ	ω:2θ	ω:2θ
scan speed	variable; 6−60 deg/min in ω	variable step scans	variable; 6−60 deg/min in ω
crystal size, mm	0.6 × 0.4 × 0.15	2.5 × 1.8 × 1.3	0.42 × 0.41 × 0.39
no. of reflns measd	8524	6521	10007
no. of reflns used	6612 ($F > 6.0\sigma(F)$)	6062	7881 ($F > 4.0\sigma(F)$)
R(F) [$R_w(F)$]^a	0.0297 [0.0368]	d	0.034 [0.036]
$R(F^2)$ [$R_w(F^2)$]^b		0.28 [0.15]	
goodness of fit^c	1.85	1.46^d	1.16
min, max peak in ΔF map, e Å^3	+0.95, −0.99	e	+1.52, −1.89

^{a} $R(F) = \Sigma\Delta/\Sigma|F_o|$; $R_w = \Sigma\Delta w^{1/2}/\Sigma|F_o|w^{1/2}$, where $\Delta = ||F_o| - |F_c||$ and $w^{-1} = \sigma^2(F) + 0.0001F^2$ for **10s**PF_6 or $w^{-1} = \sigma^2(F) + 0.0002F^2$ for **20s**BF_4. ^{b} $R(F^2) = \Sigma\Delta/\Sigma F_o^2$; $R_w(F^2) = [\Sigma w\Delta^2/\Sigma w^2F_o^4]^{1/2}$ where $\Delta = |F_o^2 - F_c^2|$, $w^{-1} = \sigma^2(F^2)$. ^{c} $S = [\Sigma(w\Delta^2)/(n - p)]^{1/2}$, where n is the number of refln used and p is the number of parameters refined. ^{d} For comparison, the $R(F)$ and $R_w(F)$ values for 2407 reflections with ($F > 3.0\sigma(F)$) are 0.102 and 0.064, respectively, with goodness of fit 1.80. ^{e} Minimum and maximum residuals were −5.3 and +8.9% of the maximum peak for the Os. These are associated with disordered phenyl rings.

An NMR spectrum recorded 1 h later did not show any change in spectral appearance and relative integral values. Observed NMR shifts: P(p-$CH_3OC_6H_4$)$_3$, −10.88 (s); [HP(p-$OCH_3C_6H_4$)$_3$]$^+$, 1.81 (d, J(H,P) = 511 Hz); *trans*-OsHBr(dppe)$_2$, 28.65 (s); *trans*-[Os(H··H)-Br(dppe)$_2$]PF_6, 17.52 (s).

No substitution reaction or coalescence of the phosphine signals is observed in the reaction of P(p-$CH_3OC_6H_4$)$_3$ with **2Os**.

X-ray Structural Characterization of 1OsPF$_6$ and 2OsBF$_4$. A green needle of **1Os**PF_6 and a pale-brown crystal of **2Os**BF_4 were mounted on glass fibers in the air, placed on a Siemens P4 diffractometer, and cooled in a stream of cold nitrogen for data collection.

A summary of selected crystallographic data are given in Table 1. Mo K$\bar{\alpha}$ radiation (λ = 0.710 73 Å) was used. For each compound the intensities of three standard reflections measured every 97 reflections showed no decay. The data were corrected for Lorentz and polarization effects and for absorption[18] (minimum and maximum transmission coefficients were 0.3785 and 0.8039 for **1Os**PF_6 and 0.5432 and 0.6438 for **2Os**BF_4).

The structures were solved and refined using the SHELXTL\PC[19] package. All non-hydrogen atoms were refined with anisotropic thermal parameters to minimize $\sum w(F_o - F_c)^2$, where $w^{-1} = \sigma^2(F) + 0.0001F^2$ for **1Os**PF_6 and $w^{-1} = \sigma^2(F) + 0.0002F^2$ for **2Os**BF_4. Hydrogen atoms were included in calculated positions and treated as riding atoms. An overall hydrogen atom thermal parameter was refined to 0.029(2) Å^2 for **1Os**PF_6 and 0.038(2) Å^2 for **2Os**BF_4. The positions of the dihydrogen atoms were determined from difference electron density maps and were refined with isotropic thermal parameters. Selected bond lengths and angles are given in Table 2. The structure of the cation **1Os**PF_6 is shown in Figure 1.

Neutron Structure Determination. Crystals were obtained by slow diffusion of Et_2O into a saturated solution of **1Os**PF_6 in CH_2Cl_2. A light-green specimen of volume 6.0 mm^3 was mounted on an aluminum pin with halocarbon grease and sealed under a helium atmosphere inside an aluminum container. This container was placed in a closed-cycle helium refrigerator and mounted on the four-circle diffractometer at port H6S of the high flux beam reactor at Brookhaven National Laboratory. The neutron beam, monochromated by Ge (220) planes in transmission geometry, was of wavelength 1.163 95(10) Å as calibrated against a KBr crystal (a_0 = 6.6000 Å at 295 K). The sample temperature was maintained at 20.0 ± 0.5 K during the experiment, and unit cell dimensions were determined by least-squares fit of sin^2(θ) values for 32 reflections in the range 41 < 2θ < 53°. Intensity data were obtained over one quadrant of reciprocal space by means of ω−2θ scans. The intensities of two reflections were monitored periodically during the data collection and showed no systematic variations throughout. Integrated intensities I_0 and variances $\sigma^2(I_0)$ were derived from the scan profiles. Lorentz factors were applied, as well as an absorption correction. Transmission factors were in the range 0.683−0.789. Averaging over 155 symmetry-related pairs of reflections resulted in an internal agreement factor of 0.072 and yielded 6113 independent observations. Further details are given in Table 1. Initial coordinates were obtained from the X-ray structure. Least-squares refinements were carried out by a full-matrix procedure,[20] minimizing $\Sigma w(F_o^2 - k^2F_c^2)^2$ using all independent data minus 51 reflections, which were affected by the powder lines from the aluminum container. The final model included the scale factor k and positional and anisotropic displacement parameters β_{ij} for all atoms, except for four P atoms and one disordered phenyl group, which were treated isotropically. Also, for some of the atoms, the cross terms β_{ij} were set to zero, since these caused the displacement tensors to go nonpositive definite, and in any case, the β_{ij} values in question did not differ significantly from zero. The isotropic type I extinction parameter[21] was omitted, since it failed to assume a significant value. This gave a total of 916 variable parameters. The refinement converged with fit indices $R(F_o^2)$ = 0.276, $R_w(F_o^2)$ = 0.151, and $R_w(F_o)$ = 0.081, S = 1.46, based on 6062 reflections. A rigid-body analysis[22] was done to correct the H−H distance for the librational motion of the H_2 ligand. The whole molecule except for the H_2 ligand was one rigid body with the H_2 ligand forming the other rigid body. The librational axis was from the Os to the

(18) Sheldrick, G. M. SHELXA-90 absorption correction program, University of Göttingen, Germany.

(19) Sheldrick, G. M. SHELXTL-PC, Siemens Analytical X-ray Instruments Inc., Madison, WI.

(20) Lundgren, J.-O. Crystallographic Computer Programs, Report UUIC-B13-4-05, Institute of Chemistry, University of Uppsala, Uppsala, Sweden, 1982.

(21) Becker, P. J.; Coppens, P. *Acta Crystallogr.* **1974**, *A30*, 129−144.

(22) Craven, B. M. Program EKRT, University of Pittsburgh, 1992.

Table 2. Selected Bond Lengths (Å) and Angles (deg) for *trans*-[Os(H··H)X($PPh_2CH_2CH_2PPh_2$)$_2$]Y (X = Cl, Y = PF_6 (**1Os**PF_6) and X = Br, Y = BF_4 (**2Os**BF_4))

	X-ray, **1Os**PF_6	neutron, **1Os**PF_6	X-ray, **2Os**BF_4
Os−HOs1	1.41(5)	1.59(2)	1.52(6)
Os−HOs2	1.67(5)	1.57(2)	1.64(6)
HOs1−HOs2	1.11(6)	1.15(3)	1.13(8)
Os−P1	2.391(1)	2.39(1)	2.414(1)
Os−P2	2.379(1)	2.39(1)	2.372(1)
Os−P3	2.382(1)	2.37(1)	2.398(1)
Os−P4	2.368(1)	2.37(1)	2.369(1)
Os−Cl (Br)	2.420(1)	2.44(1)	2.560(1)
P1−C1	1.860(5)	1.85(1)	1.849(5)
P1−C11	1.819(5)	1.83(1)	1.836(5)
P1−C21	1.832(5)	1.84(1)	1.827(5)
P2−C2	1.832(5)	1.84(1)	1.828(5)
P2−C31	1.820(4)	1.83(1)	1.816(5)
P2−C41	1.834(5)	1.85(1)	1.829(5)
P3−C3	1.843(5)	1.90(2)	1.840(4)
P3−C51	1.797(6)	1.78(2)	1.819(6)
P3−C61	1.827(5)	1.83(2)	1.820(5)
P4−C4	1.819(5)	1.84(1)	1.832(5)
P4−C71	1.825(5)	1.83(1)	1.825(5)
P4−C81	1.819(4)	1.83(1)	1.828(5)
C1−C4	1.523(6)	1.52(1)	1.521(7)
C2−C3	1.502(6)	1.48(2)	1.518(7)
Cl(Br)−Os−P1	92.5(1)	92.7(4)	91.7(1)
Cl(Br)−Os−P2	84.6(1)	84.9(4)	85.5(1)
Cl(Br)−Os−P3	86.4(1)	85.6(4)	85.6(1)
Cl(Br)−Os−P4	95.3(1)	95.2(4)	95.7(1)
P1−Os−P2	98.9(1)	99.7(4)	98.5(1)
P1−Os−P3	178.7(1)	178.1(5)	177.3(1)
P1−Os−P4	79.3(1)	78.9(4)	80.8(1)
P2−Os−P3	81.7(1)	81.1(4)	81.7(1)
P2−Os−P4	178.2(1)	178.6(5)	178.6(1)
P3−Os−P4	100.1(1)	100.3(4)	99.2(1)
Cl(Br)−Os−HOs1	158(2)	157.4(9)	151(2)
Cl(Br)−Os−HOs2	160(2)	159.9(10)	166(2)
P1−Os−HOs1	69(2)	71.8(9)	70(2)
P1−Os−HOs2	103(2)	102.7(9)	102(2)
P2−Os−HOs1	87(2)	81.8(8)	76(2)
P2−Os−HOs2	104(2)	104.8(9)	96(2)
P3−Os−HOs1	112(2)	110.1(9)	113(2)
P3−Os−HOs2	78(2)	78.8(9)	81(2)
P4−Os−HOs1	92(2)	97.7(8)	103(2)
P4−Os−HOs2	76(2)	75.6(9)	83(2)
HOs1−Os−HOs2	41(2)	42.6(12)	42(3)
Os−P1−C1	107.9(1)	108.4(6)	108.2(2)
Os−P1−C11	118.9(2)	119.0(6)	121.9(2)
Os−P1−C21	116.8(1)	117.1(6)	116.2(2)
C1−P1−C11	106.3(2)	106.1(6)	102.9(2)
C1−P1−C21	100.7(2)	101.4(7)	102.5(2)
C11−P1−C21	104.4(2)	103.0(7)	102.7(2)
Os−P2−C2	107.1(1)	107.7(6)	107.2(2)
Os−P2−C31	119.9(1)	119.6(6)	121.8(2)
Os−P2−C41	119.9(2)	119.8(6)	119.1(2)
C2−P2−C31	103.8(2)	104.4(7)	102.6(2)
C2−P2−C41	100.3(2)	100.7(6)	100.5(2)
C31−P2−C41	103.0(2)	102.1(7)	102.4(2)
Os−P3−C3	108.2(2)	109.8(7)	108.3(2)
Os−P3−C51	116.7(2)	119.1(7)	116.7(2)
Os−P3−C61	119.8(2)	119.5(7)	123.2(2)
C3−P3−C51	105.2(3)	104.5(8)	104.1(2)
C3−P3−C61	99.8(2)	95.4(8)	99.1(2)
C51−P3−C61	105.0(2)	105.0(8)	102.7(2)
Os−P4−C4	103.4(1)	104.2(6)	103.8(1)
Os−P4−C81	120.5(1)	119.3(6)	119.1(1)
Os−P4−C71	120.2(2)	121.4(6)	120.4(1)
C4−P4−C71	105.0(2)	104.5(6)	105.2(2)
C4−P4−C81	102.2(2)	101.5(6)	102.4(2)
C71−P4−C81	103.1(2)	103.3(7)	103.8(2)
P1−C1−C4	112.6(3)	113.7(7)	112.9(3)
P2−C2−C3	106.7(4)	109.0(8)	107.2(3)
P3−C3−C2	110.6(3)	108(1)	111.5(3)
P4−C4−C1	112.0(3)	110.3(7)	110.7(3)

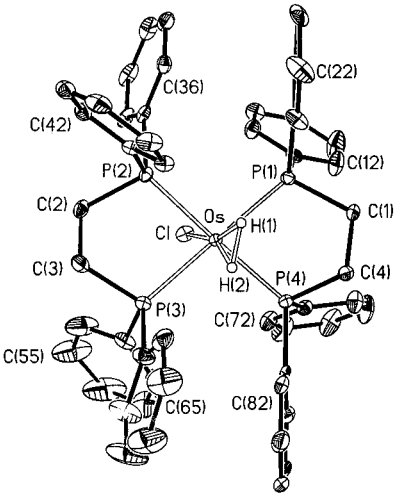

Figure 1. Molecular structure of the cation **1Os**PF_6 as determined by single-crystal X-ray diffraction.

midpoint of HOs1 and HOs2. Under these assumptions the d_{HH} lengthens from 1.15(3) to 1.22(3) Å. The core structure of **1Os**PF_6 is shown in Figure 2. Bond lengths and angles are listed in Table 2.

Results and Discussion

Starting Materials. The starting materials for the preparation of the osmium dihydrogen complexes are the complexes *trans*-$OsHXL_2$ (L = dppe, X = Cl (**10Os**), Br (**11Os**), L = depe, X = Cl (**12Os**)) or the new 5-coordinate complexes $[OsX(dppe)_2]^+$ (X = Cl (**8Os**), Br (**9Os**)). Complexes **10Os** and **12Os** were first reported by Chatt and Hayter[16] without full spectroscopic characterization, but the method of synthesis of **10Os** was difficult to reproduce. Complex **10Os** is obtained in a pure form by reacting *trans*-$[Os(H_2)H(dppe)_2]BF_4$ (**5Os**) with LiCl. The synthesis of the new complexes *cis*-$OsBr_2(dppe)_2$, and **11Os** directly from $(NH_4)_2[OsBr_6]$ represents a significant improvement in the route to dppe complexes of Os(II) in terms of number of steps and overall yield.

The complexes **8Os** and **9Os** are prepared from the dihalide complexes *cis*-$OsCl_2(dppe)_2$[13] or *cis*-$OsBr_2(dppe)_2$, respectively, as in eq 1 (X = Cl or Br). Complex **8Os** forms air-stable, red

$$cis\text{-}OsX_2(dppe)_2 + NaPF_6 \rightarrow [OsX(dppe)_2]PF_6 + NaX \quad (1)$$

crystals. The cation of **8Os** has a distorted trigonal bipyramidal structure in the solid state[15] which is almost identical to that of the ruthenium(II) analogue (**8Ru**) reported recently.[2]

Synthesis of the Complexes *trans*-[Os(H··H)X(L)$_2$]$^+$. These dihydrogen complexes are prepared by reacting complexes **8Os** or **9Os** with H_2 (1 atm) for 10 min at 20 °C in CH_2Cl_2 as in eq 2 (X = Cl (**1Os**PF_6), X = Br (**2Os**PF_6)). They are also made by reacting complexes **10Os**, **11Os**, or **12Os** with HBF_4 in ether under Ar or N_2 as in eq 3 (X = Cl, L = dppe (**1Os**BF_4); X = Br, L = dppe (**2Os**BF_4); X = Cl, L = depe (**3Os**BF_4)).

$$[OsX(dppe)_2]PF_6 + H_2 \rightarrow trans\text{-}[Os(H{\cdot\cdot}H)X(dppe)_2]PF_6 \quad (2)$$

$$trans\text{-}OsHXL_2 + HBF_4{\cdot}Et_2O \rightarrow trans\text{-}[Os(H{\cdot\cdot}H)X(L)_2]BF_4 \quad (3)$$

Reaction 2 produces **1Os**PF_6 and **2Os**PF_6 in excellent yield as light-green or pale-brown crystals, respectively. Reaction 3 produces cream-colored **1Os**BF_4, pale-brown **2Os**BF_4, or white **3Os**BF_4. These forms of **1Os** or **2Os** are soluble in CH_2Cl_2 and stable for at least 1 week under 1 atm of N_2 at 20 °C.

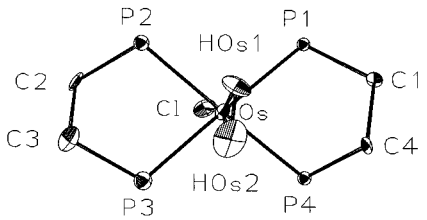

Figure 2. Structure of the core of **1Os**PF_6 as determined by neutron diffraction.

Complex **3Os**BF_4 dissolves in acetone, THF, and CH_2Cl_2 to give colorless solutions; however, these begin to decompose after 1 d. The dihydrogen complexes **1Os** and **2Os** also form in the gas phase during the FAB MS analysis of the complexes **10Os** and **11Os**; this must involve protonation reactions like eq 3 except that the nitrobenzyl alcohol solvent used in this analysis is a much weaker acid than HBF_4.

The IR spectra (Nujol mull) of **1Os**PF_6 and **1Os**BF_4 are identical and do not show any peaks in the region 3000−1800 cm^{-1} that could be assigned to Os−H or H−H stretches. The IR spectrum of **2Os**BF_4 also does not display such absorptions.

Solid-State Structure of *trans*-[Os(H··H)Cl(dppe)$_2$]PF$_6$ (1OsPF$_6$). The X-ray structure analysis shows that there is an elongated dihydrogen ligand with d_{HH} of 1.11(6) Å located trans to the chloride ligand on an octahedral osmium center. The structure from neutron diffraction at 20 K refined to give an H−H distance of 1.15(3) Å; when a correction is applied to account for the librational motion of this ligand, the H−H distance becomes 1.22(3) Å.[23] Neutron diffraction studies of dihydrogen complexes reveal that a wide range of distances is possible. Complexes with H−H distances close to the present value are $[Ru(C_5Me_5)(H_2)(dppm)]BF_4$ (1.10(2) Å),[7] *cis*-$IrCl_2(H_2)H(P^iPr_3)_2$ (1.11(3) Å),[24] $[Os(H{\cdot\cdot}H)(OAc)(en)_2]PF_6$ (1.34(2) Å),[4] and $Re(H{\cdot\cdot}H)H_5(Ptol_3)_2$ (1.357(7) Å).[25] Therefore complex **1Os** fills in the gap in this apparent continuum of distances.

The orientation of the H_2 group is staggered with respect to the P−Os−P bonds. The H atoms are between pairs of P atoms which have angles P−Os−P of about 100° and not between those with P−Os−P of about 80°, the bite angle of the dppe ligands. The X-ray and neutron studies provided identical orientations within experimental error. This is similar to the orientation of the H··H group in $[Os(H{\cdot\cdot}H)(OAc)(en)_2]^+$ where the hydrogens are between pairs of nitrogens not linked by the ethylene backbones.[4] The staggered conformation was calculated to be 2.5 kcal mol^{-1} lower in energy than the eclipsed conformation for this latter complex.[26] When the H_2 unit eclipses a *trans*-P−M−P grouping, this P−M−P angle becomes less than 180° and bent away from the H_2 ligand as in the case of *trans*-$[Fe(H_2)H(dppe)_2]BF_4$, where the P−Fe−P angle is 163.0(1)°,[27] and in the case of *trans*-$Mo(H_2)(CO)(dppe)_2$, where the P−Mo−P angle is 174.2(1)°.[28]

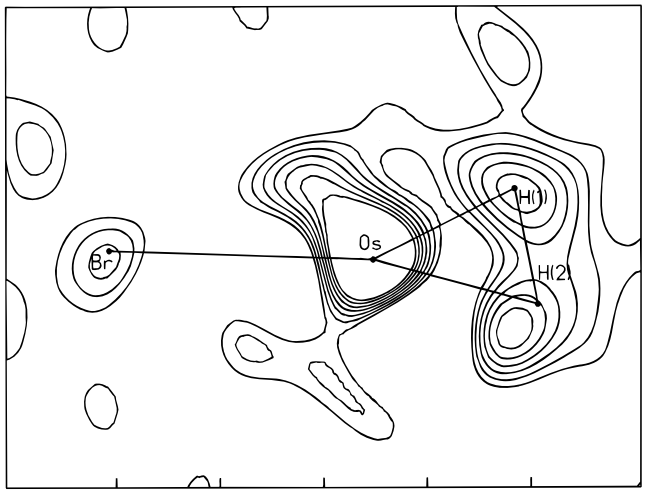

Figure 3. Final difference electron density map in the $BrOsH_2$ plane of **2Os**BF_4. Contours are shown every 0.1 e $Å^3$. The contours on Os climb in the center to 1.5 e $Å^3$ but are truncated at 0.7 e $Å^3$.

In the X-ray structure the dihydrogen ligand appears to be unsymmetrically bonded to the Os with Os−H distances of 1.41(5) and 1.67(5) Å. However this is an artifact of the experiment because the neutron study reveals essentially equivalent Os−H distances of 1.57(2) and 1.59(2) Å. The H_2 ligand in *trans*-$Re(H_2)Cl(PMePh_2)_4$ appeared to be unsymmetrically bonded in the refined model from X-ray diffraction;[29] this might also be an artifact. The complex **5Os**BF_4 has been shown in a neutron diffraction study to have a symmetrical triangular OsH_2 unit with Os−H distances of 1.71(4) and 1.77(3) Å and an H−H distance of ≥0.79 Å.[30,31] The Os−H distances are shorter for **1Os**PF_6 relative to **5Os**BF_4 because of the lower trans influence of chloride versus hydride.

The four P atoms of **1Os**PF_6 are coplanar with each other and the Os atom. The Os−P distances (2.38(1) Å on average) are systematically longer than those in **5Os**BF_4 (2.343(2) Å on average)[30,32] because of increased steric repulsions due to the chloride ligand in **1Os**PF_6 compared to the hydride ligand in **5Os**BF_4.

The PF_6^- anion inserts fluorine F(5) into the H_2 binding pocket defined by four phenyl rings. The two H··F distances are 2.68(4) Å (F5−HOs1) and 2.72(4) Å (F5−HOs2). There is an electrostatic attraction between the fluoride ($\delta-$) and acidic dihydrogen ($\delta+$) groups. However the distances are longer than the sum of van der Waals radii for hydrogen and fluorine (2.55 Å). A related interaction between a chloride ligand and the hydrogen of a dihydrogen ligand in $Ir(H_2)(H)Cl_2(P^iPr_3)_2$ has already been reported.[24]

Solid-State Structure of *trans*-[Os(H··H)Br(dppe)$_2$]BF$_4$, 2OsBF$_4$. The pale-brown crystals of this complex were isomorphous with those of **1Ru**.[2] In contrast to those of **1Ru**, data quality was sufficient to allow the refinement of the positions of the hydrogens bonded to osmium in the X-ray structure determination at 150 K. The cation is octahedral with the dihydrogen ligand positioned trans to the bromide. Figure 3 shows a difference electron density map in the $BrOsH_2$ plane.

(23) The libration of the H_2 ligand creates banana-shaped smears of nuclear density at the ends of the H−H vector. When this shape is modeled by a thermal ellipsoid, an artificially short *d*(HH) is obtained. In order to verify the correction, calculations were also performed using Maverick and Trueblood's THMA14 program which yielded a value of 1.24 Å. See ref 24.

(24) Albinati, A.; Bakhmutov, V. I.; Caulton, K. G.; Clot, E.; Eckert, J.; Eisenstein, O.; Gusev, D. G.; Grushin, V. V.; Hauger, B. E.; Klooster, W. T.; Koetzle, T. F.; McMullan, R. K.; O'Loughlin, T. J.; Pelissier, M.; Ricci, J. S.; Sigalas, M. P.; Vymenits, A. B. *J. Am. Chem. Soc.* **1993**, *115*, 7300−7312.

(25) Brammer, L.; Howard, J. A. K.; Johnson, O.; Koetzle, T. F.; Spencer, J. L.; Stringer, A. M. *J. Chem. Soc., Chem. Commun.* **1991**, 241−243.

(26) Craw, J. S.; Bacskay, G. B.; Hush, N. S. *J. Am. Chem. Soc.* **1994**, *116*, 5937−5948.

(27) Morris, R. H.; Sawyer, J. F.; Shiralian, M.; Zubkowski, J. *J. Am. Chem. Soc.* **1985**, *107*, 5581−2.

(28) Kubas, G. J.; Burns, C. J.; Eckert, J.; Johnson, S. W.; Larson, A. C.; Vergamini, P. J.; Unkefer, C. J.; Khalsa, G. R. K.; Jackson, S. A.; Eisenstein, O. *J. Am. Chem. Soc.* **1993**, *115*, 569−581.

(29) Cotton, F. A.; Luck, R. L. *Inorg. Chem.* **1991**, *30*, 767−774.

(30) Maltby, P. A.; Morris, R. H.; Klooster, W. T.; Koetzle, T. F.; Ricci, J. S.; Albinati, A. Manuscript in preparation.

(31) The H−H distance still needs to be corrected for the effects of the large amplitude of libration of the H_2 ligand.

(32) Farrar, D. H.; Maltby, P. A.; Morris, R. H. *Acta Crystallogr., Sect. C* **1992**, *C48*, 28−31.

Table 3. Observed T_1 Values of the Dihydrogen Ligands in the Complexes *trans*-$[Os(H{\cdot\cdot}H)X(L)_2]^+$ and the Methylene Protons of **1Os**[a]

1Os, 300 MHz		**1Os**, 400 MHz		**1Os**, 500 MHz		**1Os**, 400 MHz[b]	
T, K	T_1(obsd), ms	*T*, K	T_1(obsd), ms	*T*, K	T_1(obsd), ms	*T*, K	T_1(obsd) [T_1(calcd)] ms
296	63	294	79	300	88	294	0.37 [0.37]
275	53	273	66	273	73	272	0..31 [0.29]
251	41	250	57	258	68	251	0.25 [0.24]
		229	54	242	67		
226	39			231	70		
201	46	207	60	226	70	229	0.22 [0.23]
		185	74	210	80	207	0.25 [0.26]
176	70	176	81	189	99	186	0.37 [0.41]

2Os, 400 MHz				**3Os**, 400 MHz			
T, K	T_1(obsd), ms	*T*, K	T_1(obsd), ms	*T*, K	T_1(obsd), ms	*T*, K	T_1(obsd), ms
293	76	229	57	295	217	227	79
272	64	208	66	268	159	207	60
251	57	186	87	248	113	187	60

[a] Observed values reproducible to ± 2 ms; errors at 293 K are ± 2 ms, and at 180 K, ± 5 ms. The solvent is CD_2Cl_2 for all complexes except for **3Os** where acetone-d_6 was used. [b] T_1(obsd) values are for the methylene protons of the dppe backbone of **1Os**. The T_1(calcd) values were obtained by use of the parameters τ_0 and E_a for **1Os** as listed in Table 4.

The refined model gave an H−H distance of 1.13(8) Å and Os−H distances of 1.64(6) and 1.52(6) Å as indicated by the triangle in Figure 3. Within the 3σ level of the estimated standard deviations of atomic positions, a more symmetrical arrangement, in which the hydrogen atoms are positioned in the centers of the contours, is also conceivable. In this case the H−H distance lengthens to about 1.4(1) Å. Both H−H distances fall in the range calculated from the ^{1}H NMR T_1(min) measurements on the dihydrogen ligand (see below). The H_2 orientation is similar to the one in **1Os**PF_6. The BF_4 anion is located with F(2) inserted into the H_2 binding pocket with an F(2) to H(2) distance of 2.6(1) Å.

The 2.320(1) Å Os−Cl bond length in **1Os**PF_6 and the 2.560(1) Å Os−Br bond length in **2Os**BF_4 are similar to those of other Os(II) halide complexes.[33] This suggests that the H_2 ligands in these complexes do not have a high trans influence. Both the Os−Cl and the Os−Br bonds are tilted toward P(2) and P(3), as in the structure of **1Ru**, because of steric repulsions with phenyl rings on P(1) and P(4).

NMR Properties of 1Os, 2Os, and 3Os in Solution. The $^{31}P\{^1H\}$ spectra of these dihydrogen complexes in CD_2Cl_2 or acetone-d_6 solution at 295 K are singlets; the spectrum of **1Os** remains a singlet down to 176 K at 121.5 MHz. Therefore these complexes are regular octahedral or there is a low-energy exchange process which makes the P atoms equivalent.

The high-field region of the ^{1}H NMR spectra of these complexes in CD_2Cl_2 at 295 K displays a quintet at −11.44 ppm with $|J(H,P)| = 11.7$ Hz for **1Os**, at −11.46 ppm with $|J(H,P)| = 11.9$ Hz for **2Os**, and at −14.0 ppm with $|J(H,P)| = 11.8$ Hz for **3**. These quintets become less well resolved as the temperature of the samples is lowered until they become broad singlets at 400 MHz below 200 K. The chemical shift of **1Os** in CD_2Cl_2 is temperature dependent and is given by $\delta(H{\cdot\cdot}H) = -11.72 + 9.42 \times 10^{-4}(T)$, where T is in K. Simulation of the line shapes shows that the J(H,P) coupling is not affected by temperature and that the broadening at low temperature is due to the short T_2 expected for the H··H ligand. Therefore the H atoms on osmium are chemically equivalent from room temperature to low temperature and they remain coupled to four equivalent P atoms.

The T_1 values of the H atoms on Os were measured as a function of temperature, T (175−300 K), by the inversion recovery method (Table 3). Samples with the same concentration of complex were used at each spectrometer frequency; this is crucial in order to fit the data as described below. The data for complex **3Os** fit the usual "V"-shaped curve when ln T_1 is plotted against 1/T, whereas those for **1Os** and **2Os** deviate from the V shape (Figure 4). The temperature-dependent T_1 values can be calculated by use of the equation for $^1H-^1H$ dipolar relaxation with a suitable spectral density function and a temperature−dependent correlation time, $\tau_c = \tau_o e^{Ea/RT}$, as reported previously.[34] The parameters which determine the correlation time of the molecule, τ_o and E_a, should be the same as those of the corresponding ruthenium complexes as long as the concentrations of the solutions are the same (Table 4). Indeed the data for **3Os** can be fit with approximately the same parameters as those of **3Ru**[2] along with either a d_{HH} of 1.06 Å

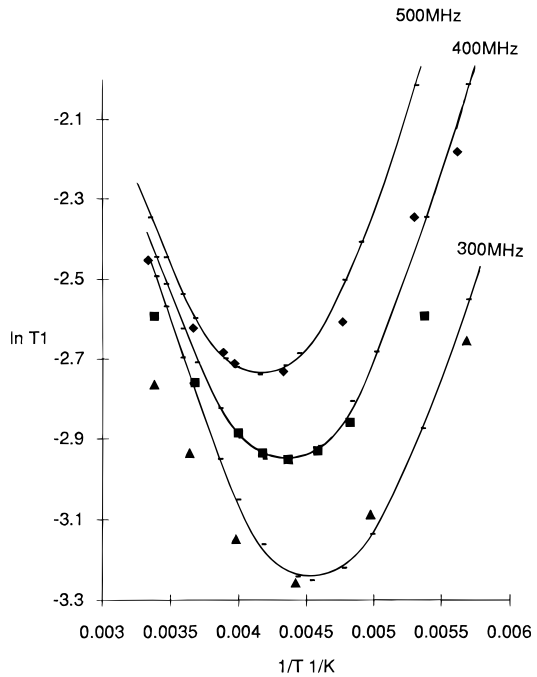

Figure 4. Plot of T_1 of the dihydrogen nuclei on a log scale versus inverse temperature for **1Os** observed at 300 (▲), 400 (■), and 500 (◆) MHz. The smooth curves are from calculated values based on d_{HH}(fast spin) = 1.04 Å or d_{HH}(slow spin) = 1.31 Å and the correlation time of the molecule given by the τ_0 and E_a parameters of the CH_2 protons of the dppe backbone (see Table 4).

(33) Orpen, A. G.; Brammer, L.; Allen, F. H.; Kennard, O.; Watson, D. G.; Taylor, R. *J. Chem. Soc., Dalton Trans.* **1989**, S1.

(34) Bautista, M. T.; Earl, K. A.; Maltby, P. A.; Morris, R. H.; Schweitzer, C. T.; Sella, A. *J. Am. Chem. Soc.* **1988**, *110*, 7031−7036.

Table 4. Parameters Used To Fit the Temperature Dependence of the T_1 Values of Complexes **1Os**, **2Os**, and **3Os** (Table 3) and **1Ru**, **3Ru**, **5Os**, and **6Os**

complex	T(min), K	T_1(min)[a] ms	$\tau_{o,\,ps}$	E_a, kcal/mol	spinning rate[b]	d_{HH}, Å min[c]	d_{HH}, Å corr[d]
1Os	230	53 ± 1	1.1[e]	2.5[e]	fast[f]	1.04	1.08
	230	53 ± 1	1.1[e]	2.5[e]	slow[f]	1.31	1.35
1Ru	240	25 ± 1	1.8	2.4	fast	0.92	0.94
2Os	238	57 ± 1	1.7	2.3	fast[f]	1.05	1.08
	238	57 ± 1	1.7	2.3	slow[f]	1.33	1.36
3Os	210	60 ± 1	0.34	2.6	fast	1.06	1.10
	210	60 ± 1	0.34	2.6	slow	1.34	1.38
3Ru	210	28 ± 1	0.37	2.7	fast	0.94	0.96
5Os	233	40 ± 1	0.90	2.6	fast	0.98	1.02
6Os	203	80 ± 1	0.19	2.9	fast[g]	(1.12)[g]	(1.17)[g]

[a] The observed minimum T_1 value, T_1(min), for the dihydrogen ligand (at temperature, T(min), and 400 MHz) obtained by direct observation and fitting to the temperature-dependent T_1 equation using a temperature dependent correlation time $\tau_c = \tau_o e^{E_a/RT}$.[34] [b] A fast rotational frequency of the H_2 unit is ≫400 MHz, while a slow frequency is ≪400 MHz. [c] Obtained from fitting the T_1 data. [d] Corrected for the relaxation contributions from neighboring protons.[35] [e] Parameters obtained by fitting the T_1 data of CH_2 groups of the dppe backbone (Table 3 and unpublished data for 300 and 500 MHz). [f] Actually an intermediate motion of the H_2 of frequency ≈ 400 MHz is suspected (see text). [g] Actually fast-spinning (H_2) and static $(H)_2$ forms are proposed to be in rapid equilibrium.

for a fast spinning ligand or 1.34 Å for a slow spinning ligand; the calculated T_1 values are listed in Table 3, and the calculated d_{HH} values are listed in Table 4. These are the minimum values of d_{HH}; to obtain the actual values the relaxation rates have to be corrected for the contributions of the ethyl group protons by the method of Desrosiers et al.[35] The resulting distances, which are slightly longer, are also listed in Table 4.

The unusual temperature dependence of the T_1 data at three different spectrometer frequencies for the dihydrogen ligand of complex **1Os** is demonstrated in Figure 4. The smooth curves are calculated using d_{HH}(slow spinning) = 1.31Å or d_{HH}(fast spinning) = 1.04 Å and the standard spectral density functions. For these calculations the parameters $\tau_0 = 1.08$ ps and $E_a = 2.5$ kcal mol^{-1} which give the correlation times for the molecule at each temperature (Table 4) were determined from the T_1 values of the methylene hydrogens of the dppe backbone (Table 3). These were similar to the correlation times calculated by use of the parameters for **1Ru** (Table 4). For a given spectrometer frequency the observed T_1 values of the dihydrogen ligand of **1Os** are shorter than expected at both high temperatures and low temperatures (Figure 4). The deviations are caused by an H_2 correlation time or rotational frequency which is near the correlation time or tumbling frequency of the complex. We attempted to model the dipolar relaxation by assuming that the correlation time of the H_2 ligand can be expressed in the exponential form $\tau_{H_2} = \tau_{rot} e^{E_{rot}/RT}$. We used the spectral density function for the case of dipolar relaxation of H_2 perpendicular to the axis of rotation (eq 4)[34] and varied d_{HH}, τ_{rot} and E_{rot}.

$$J(\omega) = 0.25\tau_c/(1 + \omega^2\tau_c^2) + 0.75(\tau_c/(2 + \tau_{H_2}/\tau_c))/(1 + \omega^2(\tau_c/(2 + \tau_{H_2}/\tau_c))^2) \quad (4)$$

Values of d_{HH} = 1.06 Å, τ_{rot} = 0.3 ps, and E_{rot} = 1.5 kcal mol^{-1} gave a reasonable fit to the 500 MHz data but did not fit all the 400 and 300 MHz data. We also tried the "model-free" spectral density function suggested by Lipari and Szabo (eq 5).[36a] The

$$J(\omega) = S^2\tau_c/(1 + \omega^2\tau_c^2) + (1 - S^2)(\tau')/(1 + \omega^2(\tau')^2) \quad (5)$$

function has a factor S^2 which ranges from 1 (no internal motion) to 0.25 (fast spinning) while $1/\tau' = 1/\tau_c + 1/\tau_{H_2}$. By use of d_{HH} = 1.22 Å from the neutron study, we determined that S^2 is approximately 0.6, which suggests the existence of an intermediate frequency of motion of the H_2. However, eq 5 with S^2 = 0.6 did not fit well to all the temperature-dependent T_1 data. A more complex physical model needs to be developed to analyze this and future data for this interesting case of intermediate motion of the H_2 ligand.[36b]

Therefore, the flattened shape of the ln T_1 versus $1/T$ plots is an indicator that the motion or motions of the H_2 ligand have frequencies similar to that of the overall motion of the molecular complex. In such a situation the actual d_{HH} will be between the values calculated from the T_1(min) value for "fast spinning" and "slow spinning". These limiting values are listed in Table 4 for **1Os** and **2Os**.

Preparation and Properties of the Deuterated Complexes. The complex *trans*-[Os(H··D)Cl(dppe)$_2$]$^+$ (**1Os**-d_1) was prepared by reacting **10Os** with $HBF_4 \cdot Et_2O$ in excess D_2O/ether or by reacting **8Os** with HD gas (generated by reacting D_2O with NaH). Some **1Os** contaminated the first sample. The ^{1}H NMR spectrum observed at 298 K is a 1:1:1 triplet of quintets at 0.013 ppm upfield of the resonances for **1Os** with J(H,P) = 11.7 Hz and J(H,D) = 13.9 ± 0.2 Hz for **1Os**-d_1 in CD_2Cl_2 and J(H,P) = 11.7 Hz and J(H,D) = 14.4 ± 0.2 Hz for **1Os**-d_1 in acetone-d_6. The J(H,D) values are also temperature dependent, decreasing with decreasing temperature (Table 5). The isotopomers **1Os** and **1Os**-d_1 appear as two closely spaced singlets at 20.8 and 20.7 ppm, respectively, in the ^{31}P{^{1}H} NMR spectrum. Complex **2Os**-d_1 gives a very similar ^{1}H NMR spectrum with J(H,P) 11.9 Hz and J(H,D) 13.7 Hz.

The complex **3Os** is enriched in deuterium by slow exchange with acetone-d_6. **3Os**-d_1 gives a pseudo-septet at −13.83 ppm, 0.016 ppm upfield of and superimposed on the (H··H) signal for **3Os**. The ^{1}H resonances of **3Os**-d_1 were observed by use of an inversion recovery experiment with a delay time of 150 ms at 400 MHz to null out the resonances of **3Os** (see refs 2, 37, and 38 for similar experiments). The null time corresponds to a T_1 for **3Os** of 217 ms (=150/ln(2)), which is in agreement with other determinations of T_1 (see Table 3). The observed intensities of the lines of the (H··D) septet are 0.7:4.8:11:14:11:4.8:0.7, close to the expected 1:5:11:14:11:5:1 pattern if J(H,D) ≈ J(H,P). The outer peak separation of 73.2 Hz corresponds to a J(H,D) coupling of 13.1 Hz, assuming that J(H,P) for **3Os**-d_1 is identical to the **3Os** value of 11.8 Hz.

Correspondence of J(H,D) and d_{HH}. We find that a plot of J(H,D) versus d_{HH} for complexes whose H−H distances have been determined by single-crystal neutron diffraction, X-ray diffraction, or solid-state NMR techniques (Table 6) gives a straight line:

$$d_{HH} = -0.0167J(H,D) + 1.42 \quad (6)$$

One complex whose parameters deviate from this plot is Ir(H$_2$)HCl$_2$(P^{i}Pr$_3$)$_2$, which may not have the same hydrogen−chlorine interaction in solution that it does in the crystal as has been discussed previously.[7] Equation 6 probably does not hold for J(H,D) < 3 Hz because *cis*-dihydride complexes with d_{HH}

(35) Desrosiers, P. J.; Cai, L.; Lin, Z.; Richards, R.; Halpern, J. *J. Am. Chem. Soc.* **1991**, *113*, 4173−4184.

(36) (a) Lipari, G.; Szabo, A. *J. Am. Chem. Soc.* **1982**, *104*, 4559−4570. (b) This model should include a treatment of the H_2 libration.

(37) Chinn, M. S.; Heinekey, D. M.; Payne, N. G.; Sofield, C. D. *Organometallics* **1989**, *8*, 1824−1826.

(38) Bautista, M. T.; Cappellani, E. P.; Drouin, S. D.; Morris, R. H.; Schweitzer, C. T.; Sella, A.; Zubkowski, J. *J. Am. Chem. Soc.* **1991**, *113*, 4876−4887.

Table 5. J(H,D) Values for $[Os(H{\cdot\cdot}D)Cl(dppe)_2]^+$ as a Function of Solvent and Temperature from 500 MHz ^{1}H NMR Spectra

1Os-d_1 in CD_2Cl_2		**1Os**-d_1 in acetone-d_6	
T, K	J(H,D), Hz	T, K	J(H,D), Hz
253	13.6	253	13.8
263	13.8	273	14.2
273	13.9	298	14.4
283	13.7	308	14.5
298	13.9		
308	14.2		

Table 6. H−H Distances of Dihydrogen Complexes in the Solid State and J(H,D) from Solution ^{1}H NMR Studies

complex	d_{HH}, Å	method[a]	J(H,D), Hz	ref
$Cr(H_2)(CO)_3(P^iPr_3)_2$	0.85	s	35	45
$[Fe(H_2)H(dmpe)_2]BPh_4$	0.86	X	31	46, 47
$[Fe(H_2)H(dppe)_2]BPh_4$	0.88	s	32	48, 49
$Mo(H_2)(CO)(dppe)_2$	0.88	s	34	28
$W(H_2)(CO)_3(P^iPr_3)_2$	0.89	s	33.5	50, 51
$[Ir(H_2)H(bq)(PPh_3)]^+$	0.94	s	29.5	49, 52
$[Ru(H_2)Cp(CO)(PCy_3)]^+$	0.97	s	28	49, 53
$[Ru(H_2)Cp(dmpe)]^+$	1.02	s	22	49, 53
$[Ru(H_2)Cp(dppm)]^+$	1.01	X	21.9	54
$[Ru(H{\cdot\cdot}H)Cp^*(dppm)]BF_4$	1.10(2)	n	20.9	7
cis-$Ir(H{\cdot\cdot}H)HCl_2(P^iPr_3)_2$	1.11(3)	n	12	24
$[Os(H{\cdot\cdot}H)Br(dppe)_2]PF_6$	1.13(8)	X	13.7	this work
$[Os(H{\cdot\cdot}H)Cl(dppe)_2]PF_6$	1.22(3)	n	13.9	this work
$[Os(H{\cdot\cdot}H)(en)_2(OAc)]PF_6$	1.34(2)	n	9.1	4
$[Os(H{\cdot\cdot}H)Cl(en)_2]PF_6$	1.39(10)	X	7.2	4
HD(g)	0.74		43	

[a] n = neutron diffraction, X = X-ray diffraction, s = solid-state NMR.

of 2 Å have J(H,H) values of at least 10 Hz which correspond to J(H,D) of up to 2 Hz. Therefore the plot should curve to higher d_{HH} at small J(H,D) values.

Equation 6 appears to provide the best estimate of d_{HH} in solution for a dihydrogen complex when J(H,D) is known. As mentioned above, the T_1 method gives ambiguous values of d_{HH} which depend on the interpretation of the motion of the H_2 ligand. However an analysis of the d_{HH} values at the fast and slow spin limits of 64 complexes which also have measured J(H,D) values shows that eq 6 could apply to all of these (see supporting information). In several cases it can be decided whether the complexes have fast-spinning or slow-spinning H_2 ligands. In general the complexes with fast-spinning H_2 ligands have hydride as the trans ligand. There is no obvious correlation apparent as yet on the nature of the trans ligand for the complexes which have slow-spinning H_2 ligands. The d_{HH} values calculated by use of eq 6 for complexes **1Os**−**6Os** and their ruthenium analogs are listed in Table 7. It appears that complexes **1Os** and **2Os** have H−H distances in solution which are between the fast- and slow-spinning limits. The rectangular bar in Figure 5 shows these extreme d_{HH} values for **1Os** as well as the limits of J(H,D) observed at high and low temperature. Therefore the d_{HH} for **1Os** in solution is likely to be about 1.20 Å as indicated by the intersection of this bar with the line from the J(H,D) values and the point from the neutron-derived solid-state distance. Similarly the d_{HH} for **2Os** must also be around 1.2 Å.

Comparison of *trans*-$[M(H_2)X(L)_2]^+$ Spectral Data and H−H Distances in Solution. Table 7 outlines the changes that occur when the trans ligand is changed from halide to hydride on osmium and ruthenium for three chelating diphosphine ligands. The bidentate ligands push more electron density onto the metal as dppe (R = Ph) < depe (R = Et) < dcpe (R = Cy). This is clearly indicated by the C−O stretching frequencies for some complexes *trans*-$[M(CO)X(L)_2]^+$ of Table 7 which decrease with this order of ligands. It is also of interest to note that ν(CO) values are lower when CO is trans to chloride than when trans to hydride. In each series of complexes with the same metal and trans ligand there is an apparent increase in the H−H distance (except possibly for the Ru complexes) and a decrease in the J(H,D) coupling of the *trans*-$[M(HD)X(L)_2]^+$ isotopomers with this order of ligands. Such a trend would be expected since an increase in π-basicity of the metal along this series would result in increased $M(d\pi) \rightarrow H_2(\sigma^*)$ back-bonding. Associated with a lengthening of the H−H bond is an increase in the coupling, J(H,P), which in turn probably indicates an increase in hydride character of the H··H unit.

The most interesting effect of halide versus hydride is the comparison of H−H distances in the series **1Os**−**4Os** versus **5Os**−**7Os**. In the former series the character of the H··H unit changes only slightly while in the latter there is a large structural change on going from a spinning dihydrogen ligand in **5Os** to a dihydride unit in **7Os**. It appears that the halide ligand buffers the effect of the phosphine ligands so that the H−H bond only lengthens a little when the electron-donor strength of the phosphine ligand increases from dppe to dcpe. As noted above, the Os−P bonds in **1Os** are longer than those in **5Os** and this might reduce the transmission of electronic influences from the substituents on phosphorus to the metal. A result of this buffering effect is that, although there is an *increase* in H−H distance on going from *trans*-$[Os(H_2)H(dppe)_2]^+$ to *trans*-$[Os(H{\cdot\cdot}H)Cl(dppe)_2]^+$, there is a *decrease* for the corresponding pair of dcpe complexes. This contrasts with the results for ruthenium where a change of the trans ligand from hydride to chloride always results in an increase in H−H distance and in the hydride character of the dihydrogen ligand.[2] It is possible that the splitting of the H−H bond in complex **4Os** and in *trans*-$[Os(H{\cdot\cdot}H)Cl(en)_2]^+$ (see Table 6) is arrested because of first coordination sphere repulsions with the chloride ligand. This might also be the explanation for why replacement of the chloride in the dihydrogen complex, $Ir(H_2)ClH_2(PPr^i_2)_2$,[39] with hydride to give the pentahydride, $IrH_5(PPr^i_3)_2$,[40] results in the breaking of the H−H bond. However a more likely explanation in this case is that octahedral $Ir(H_2)H_3(PPr^i_3)_2$ is expected to be high in energy because it is forced to have trans hydride ligands.[41]

It is also possible that **1Os**−**4Os** exist as mixtures of dihydrogen complexes and dihydride complexes which are in rapid equilibrium as has been proposed for **6Os**.[5] Then the observed NMR properties of the complexes ($\delta(H_2)$, δ(P), J(H,P), J(H,D), $T_1(H_2)$) would be the weighted average of those of the two forms. The low-temperature (180 K) ^{1}H and ^{31}P spectra do not give evidence for two species. The increase in J(H,D) of **1Os**-d_1 with increasing temperature, as is also observed for **4Os**-d_1,[5] provides evidence for such a rapid equilibrium where the equilibrium shifts more from the Os(H)(D) species toward the Os(HD) one with increasing temperature. It is difficult to explain the increase in J(H,D) with a single species since an increase in thermal motion of an elongated H··D ligand might be expected to result in a decrease in J(H,D) with increasing temperature as observed for the complex $[Ru(C_5Me_5)(H{\cdot\cdot}H)(dppm)]^+$.[7] Other possible evidence for a rapid equilibrium is the observation of the temperature dependence of the chemical shift of the dihydrogen ligand and the observation of disorder in one dppe ligand in the X-ray structure of **1Os**BF_4 which might

(39) Mediati, M.; Tachibana, G. N.; Jensen, C. M. *Inorg. Chem.* **1992**, *31*, 1827−1832.

(40) Garlaschelli, L.; Khan, S. I.; Bau, R.; Longoni, G.; Koetzle, T. F. *J. Am. Chem. Soc.* **1985**, *107*, 7212−7213.

(41) Eisenstein, O. Personal communication.

Table 7. Spectroscopic Properties and H−H Distances of Dihydrogen Complexes of the Type *trans*-[M(H··H)XL$_2$]$^+$

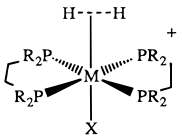

M	H$_2$	X	R on P	T_1 (min) at 400 MHz, ms	d_{HH} from T_1, Å	^1J(H,D), Hz	d_{HH} from J(H,D), Å	^2J(H,P), Hz	*trans*-[M(CO)XL$_2$]$^+$ ν(CO) cm^{-1}
1Os	H··H	Cl	Ph	53	1.08−1.35	13.9[a]	1.19	11.7	1936[b]
2Os	H··H	Br	Ph	57	1.08−1.36	13.7	1.19	11.7	
3Os	H··H	Cl	Et	60	1.1−1.4	13.1	1.20	11.7	
4Os[c]	H··H	Cl	Cy	50	1.1−1.4	10.5	1.24	12.8	1917[d]
5Os	H$_2$	H	Ph	40	1.02	25.5	0.99	5	2003[e]
6Os	H··H	H	Et	80	1.2−1.5	11.5[a]	1.23	5.5	1974[f]
7Os[c]	(H)$_2$	H	Cy	175[g]	>1.6			10.4[g]	1975,[h] 1875[h]
1Ru[i]	H$_2$	Cl	Ph	25	0.94−1.2	25.9	0.99	7.4	1946[j]
3Ru[i]	H$_2$	Cl	Et	28	0.96−1.2	25.2	1.00	7.2	
4Ru[c]	H··H	Cl	Cy	20	0.94−1.2	16	1.15	8	1940[k]
5Ru[l]	H$_2$	H	Ph	20	0.90	32.0	0.88		1987[m]
6Ru[l]	H$_2$	H	Et	16	0.85	32.3	0.88		1958[f]
7Ru[c]	H$_2$	H	Cy	15	0.84	31.5	0.89		

[a] J(H,D) solvent and temperature dependent. [b] Reference 55. [c] The T_1 values from ref 3 had to be scaled from 80 to 400 MHz to provide this comparison. The calculation of H−H distances for these complexes has larger uncertainty because of the less accurate 80 MHz T_1 data and the problem that the bidentate ligands have several protons that can contribute to the relaxation of the metal-bonded hydrogens. [d] Reference 56. [e] Reference 5. [f] Reference 57. [g] Values averaged with those of the terminal hydride due to rapid intramolecular H-atom exchange. [h] Mixed ν(OsH) and ν(CO) modes. Reference 3. [i] Reference 2. [j] Reference 58. [k] Reference 59. [l] Reference 38. [m] Reference 60.

be explained by the cocrystallization of dihydride and dihydrogen isomers.[17] The anomalously short T_1 values at low temperatures (Figure 4, 400 and 500 MHz) are not explained by such an equilibrium since lower temperatures should result in a shift in the postulated equilibrium to the Os(H)$_2$ form which would have a longer T_1.

The actual description of complexes **1Os**−**3Os** is probably neither an elongated dihydrogen complex with a fixed H−H distance nor a rapid equilibrium but instead complexes with two H atoms moving rapidly in flat potential wells with shallow minima at the crystallographically determined positions where the H−H separation is about 1.2 Å.

Acidity of 1Os and 2Os. Complex **1Os** is not deprotonated by PEtPh$_2$ in CH$_2$Cl$_2$. This contrasts with **1Ru** which is partially deprotonated by PEtPh$_2$ and is in equilibrium with HPEtPh$_2^+$ (pK_a 4.9) and **10Ru**.[2] Therefore **1Os** is less acidic than **1Ru**, which has a pK_a of 6.0. The osmium complex is partially deprotonated by PMe$_2$Ph and in equilibrium with HPMe$_2$Ph$^+$ (pK_a 6.5) and **10Os** (eq 7, K = 0.12, 293 K). Therefore the

$$\underset{\textbf{1Os}}{\textit{trans}\text{-[Os(H··H)Cl(dppe)}_2\text{]}^+} + \text{PMe}_2\text{Ph} \overset{K}{\rightleftharpoons} \underset{\textbf{10Os}}{\textit{trans}\text{-OsHCl(dppe)}_2} + \text{HPMe}_2\text{Ph}^+ \quad (7)$$

pK_a of **1Os** is determined to be 7.4 ± 0.3. This is much more acidic than the complex with hydride trans to dihydrogen— the pK_a of **5Os** is 13.6 ± 0.3.[42] This large difference in acidity can be attributed to the stronger H−H interaction in **5Os** and the stronger electron-donor ability of hydride versus halide (see below).

Complex **2Os** is partly deprotonated by P(p-CH$_3$OC$_6$H$_4$)$_3$ and is in equilibrium with HP(p-CH$_3$OC$_6$H$_4$)$_3^+$ (pK_a 4.57) (eq 8, R = p-CH$_3$OC$_6$H$_4$, K = 0.155, 293 K). The pK_a of **2Os** is therefore 5.4±0.3. The fact that **2Os** is more acidic than **1Os** is consistent with the fact that **1Os** is not deprotonated at all by P(p-CH$_3$OC$_6$H$_4$)$_3$.

(42) Cappellani, E. P.; Drouin, S. D.; Jia, G.; Maltby, P. A.; Morris, R. H.; Schweitzer, C. T. *J. Am. Chem. Soc.* **1994**, *116*, 3375−3388.

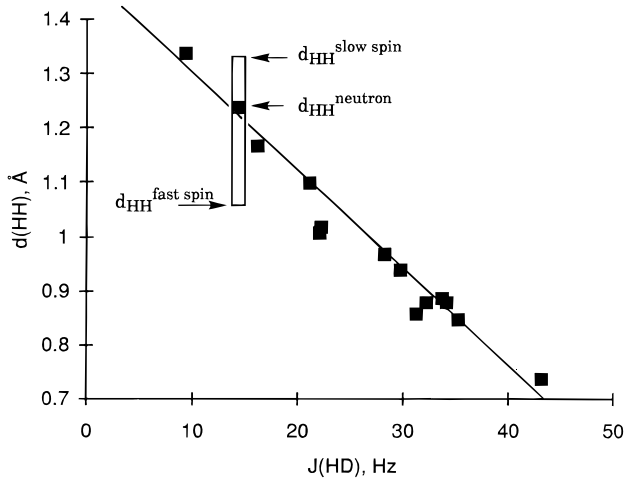

Figure 5. Plot of d_{HH} versus J(H,D) for dihydrogen complexes. The filled squares are the data from Table 6 except for those of the iridium complex. The rectangular bar represents the limits of d_{HH} determined for the T_1 data for **1Os** (see Table 4).

$$\underset{\textbf{2Os}}{\textit{trans}\text{-[Os(H··H)Br(dppe)}_2\text{]}^+} + \text{PR}_3 \overset{K}{\rightleftharpoons} \underset{\textbf{11Os}}{\textit{trans}\text{-OsHBr(dppe)}_2} + \text{HPR}_3^+ \quad (8)$$

In summary, pK_a values for complexes *trans*-[Os(H··H)X(dppe)$_2$]$^+$ increase with the trans X$^-$ligand as Br$^-$ (5.4) < Cl$^-$ (7.4) < H$^-$ (13.6). The same trend is observed in the enthalpy of protonation of the complexes Os(C$_5$H$_5$)(PPh$_3$)$_2$X to give hydrides [OsH(C$_5$H$_5$)X(PPh$_3$)$_2$]$^+$ where $-\Delta H_{HM}$ increases with X$^-$ in the order I$^-$ (14.1 kcal mol^{-1}) < Br$^-$ (16.3) < Cl$^-$ (19.7) < H$^-$ (37.3). Note that the trend for the halides is opposite to that expected on the basis of the electronegativity of the substituent. Angelici has explained this effect of X$^-$ on the acidity of osmium monohydride or dihydride complexes in terms of the donor abilities of the X$^-$ ligands as reflected in their gas-phase proton affinities which correlate exactly with $-\Delta H_{HM}$.[43]

The electrochemical potentials $E°$(Os^{3+}/Os^{2+}) of **10Os** and **11Os** are −0.14 and −0.11 V vs Fc$^+$/Fc, respectively.[14,38] The

(43) Angelici, R. J. *Acc. Chem. Res.* **1994**, *28*, 51−60.

Table 8. Dependence of Acidity (pK_a) and M−H Bond Dissociation Energy on the H−H Distance of Dihydrogen and Dihydride Complexes

complex	d_{HH}, Å from J(H,D)	pK_a	ΔH_{BDE}, kcal/mol	ref
$[Os(H_2)H(dppe)_2]^+$, **5Os**	1.0	13.6	80 ± 1	42
$[Os(H{\cdot\cdot}H)Cl(dppe)_2]^+$, **1Os**	1.2	7.4	73 ± 1	this work
$[Os(H{\cdot\cdot}H)Br(dppe)_2]^+$, **2Os**	1.2	5.4	71 ± 1	this work
$[Ru(H_2)H(dppe)_2]^+$, **5Ru**	0.9	15.0	82 ± 2	42
$[Ru(H_2)Cl(dppe)_2]^+$, **1Ru**	1.0	6.0	71 ± 3	2
$[RuH_3(dppfc)_2]^+$ [a]	>1.8	4.4	58 ± 2	2
$[Cp^*Ru(H{\cdot\cdot}H)(dppm)]^+$	1.1	9.2	73 ± 2	42, 61
$[Cp^*RuH_2(dppm)]^+$	>1.8	8.8	72 ± 2	42, 61

[a] dppfc = 1,1′-bis(diphenylphosphino)ferrocene.

pK_a and $E°$ values can be used to calculate the energy required to remove an H atom from **1Os** and **2Os**, $\Delta H_{BDE} = 73 \pm 1$ and 71 ± 1 kcal mol^{-1}, respectively.[42] By contrast the comparable energy for **5Os** is 80 ± 1 kcal mol^{-1}.[42] Again these H atom abstraction energies parallel those calculated from $-\Delta H_{HM}$ for the hydride complexes $[OsHX(C_5H_5)(PPh_3)]$: 63.2 (Br^-), 66.4 (Cl^-), 73.6 (H^-) kcal mol^{-1}.[44] The unusually large BDE value for **5Os** might be a result of some H−H bonding as well as Os−H bonding since this complex has the shortest H−H distance (1.0 Å versus about 1.2 Å for **1Os** and **2Os** and >1.6 Å for $[OsH_2(C_5H_5)(PPh_3)]^+$).

Some ΔH_{BDE} values that have been determined so far are listed in Table 8. There is a trend developing such that ,as the H−H bond stretches past 1.0 Å, the energies drop to values expected for metal dihydrides. Therefore, even though the hydrogens are still close together at 1.1−1.2 Å, they have the acidity of dihydrides or, in other words, their acidity is not influenced by H−H bonding. In the few instances where it has been determined, osmium hydride complexes are less acidic than comparable ruthenium hydride complexes.[42] This is also true in a comparison of **1Os** and *trans*-$[Ru(H{\cdot\cdot}H)Cl(dppe)_2]^+$ (Table 8) with pK_a values of 7.4 and 6.0, respectively. The complexes *trans*-$[M(H_2)H(L)_2]^+$ are the exception to this rule where the ruthenium complexes are less acidic than the osmium complexes because of the stronger H−H bonds in the former.[42]

Conclusions

We propose that the new octahedral complexes *trans*-$[Os(H{\cdot\cdot}H)X(L)_2]^+$ (L = dppe, X = Cl, Br, L = depe, X = Cl), have elongated dihydrogen ligands in the range of 1.1−1.22 Å in the solid-state and in solution. The distances are established in the solid-state by X-ray diffraction for the dppe complexes and neutron diffraction for **1Os**PF_6. Therefore these complexes are classified as having stretched or elongated dihydrogen ligands, arrested along the pathway to homolytic splitting or oxidative addition.[10] However it is likely that the hydrogen atoms are moving rapidly in a flat potential surface above the OsP_4 plane and that this elongated separation is at a shallow minimum on this surface. The temperature and solvent dependence of J(H,D) noted for **1Os**-d_1 might be evidence for the flat potential energy well and large excursions from equilibrium positions of the H and D.

The distances in solution are more difficult to obtain. An approximate d_{HH} can be obtained from the coupling J(H,D) by use of eq 6. The method of determining the T_1(min) value of the ^{1}H nuclei of the dihydrogen ligand provides upper and lower limits for d_{HH}. However the correct spectral density function to describe the motion of the H··H ligand is needed to derive a reliable d_{HH} value. We describe for the first time how the deviations in T_1 values of the H_2 ligand from those expected on the basis of the correlation time of the molecule signal the case of hindered spinning of the H··H ligand. However a suitable spectral density function to define the motion of the H_2 ligand and allow a fit to all the T_1 data has not yet been found.

The hindered motion when dihydrogen is trans to Cl and Br in **1Os**−**3Os** contrasts with the fast spinning when dihydrogen is trans to hydride in complexes *trans*-$[M(H_2)HL_2]^+$ (M = Fe, Ru, Os).[38] The H−H distances of the latter complexes are short (in the range 0.85−1.0 Å) and the M−H_2 interaction is weak because of the high trans influence of the hydride which weakens Os ← H_2 σ-bonding and the strong ligand field splitting effect of hydride which lowers the Os($d\pi$) electron energies and decreases Os → π back-donation. Craw and Hush[26] have explained the stretching of the dihydrogen ligands in the series of complexes *trans*-$[Os(H{\cdot\cdot}H)L(NH_3)_4]^{n+}$ as a function of a spectrochemical parameter for L which expresses this ligand field splitting concept. This explains why the weaker field halide ligands cause longer d_{HH} distances and smaller J(H,D) couplings in such complexes relative to the hydride ligand.

We note that there is a "buffering effect" of the trans halide on the transmission of electron density from the cis chelating phosphines to the dihydrogen ligand via Os($d\pi$) → H_2(σ*) back-donation. For the case of chloride trans to dihydrogen, there is a moderate increase in d_{HH} on going from the less donating dppe ligand (1.22 A) in **1Os** to the more donating dcpe (1.3 Å) in **4Os**, while in the case of hydride trans to dihydrogen, the dppe complex **5Os** has d_{HH} of 1.0 Å and the dcpe complex **7Os** has no H−H bonding (d_{HH} > 1.6 Å). This effect is attributed to a weakening of Os−P bonding by the halide ligand which is reflected in the longer Os-P bond distances of **1Os** and **2Os** compared to **5Os**.

There is clearly a continuum of d_{HH} of dihydrogen complexes ranging from 0.85 to 1.4 Å (Table 6). The osmium complexes of Table 6 make an interesting series of structures with seven donor atoms on the metal starting with octahedral Os(II) complexes with short d_{HH} and proceeding to structures which are intermediate in the oxidative addition to Os(IV), 7-coordinate complexes. It is likely that other complexes in Table 6 and others in the literature have unsymmetrical T_1 versus $1/T$ behavior because of hindered motion of the H··H ligand. It is

(44) Wang, D.; Angelici, R. J. *J. Am. Chem. Soc.* **1996**, *118*, 935−942.
(45) Kubas, G. J.; Nelson, J. E.; Bryan, J. C.; Eckert, J.; Wisniewski, L.; Zilm, K. *Inorg. Chem.* **1994**, *33*, 2954−2960.
(46) Baker, M. V.; Field, L. D.; Young, D. J. *J. Chem. Soc., Chem. Commun.* **1988**, 546−548.
(47) Hills, A.; Hughes, D. L.; Jimeneztenorio, M.; Leigh, G. J.; Rowley, A. T. *J. Chem. Soc., Dalton Trans.* **1993**, 3041−3049.
(48) Ricci, J. S.; Koetzle, T. F.; Bautista, M. T.; Hofstede, T. M.; Morris, R. H.; Sawyer, J. F. *J. Am. Chem. Soc.* **1989**, *111*, 8823−8827.
(49) Zilm, K. W.; Millar, J. M. *Adv. Magn. Opt. Reson.* **1990**, *15*, 163−200.
(50) Kubas, G. J.; Unkefer, C. J.; Swanson, B. I.; Fukushima, E. *J. Am. Chem. Soc.* **1986**, *108*, 7000−7009.
(51) Zilm, K. W.; Merrill, R. A.; Kummer, M. W.; Kubas, G. J. *J. Am. Chem. Soc.* **1986**, *108*, 7837−7839.
(52) Crabtree, R. H.; Lavin, M.; Bonneviot, L. *J. Am. Chem. Soc.* **1986**, *108*, 4032−4037.
(53) Chinn, M. S.; Heinekey, D. M. *J. Am. Chem. Soc.* **1990**, *112*, 5166−5175.
(54) Heinekey, D. M.; Oldham, W. J. *Chem. Rev.* **1993**, *93*, 913−926.
(55) Smith, G.; Cole-Hamilton, D. J.; Thorton-Pett, M.; Hursthouse, M. B. *J. Chem. Soc., Dalton Trans.* **1985**, 387−393.
(56) Mezzetti, A.; Del Zotto, A.; Rigo, P. *J. Chem. Soc., Dalton Trans.* **1990**, 2515−2520.
(57) Bancroft, G. M.; Mays, M. J.; Prater, B. E.; Stefanini, F. P. *J. Chem. Soc. (A)* **1970**, 2146−2149.
(58) Smith, G.; Cole-Hamilton, D. J. *J. Chem. Soc., Dalton Trans.* **1984**, 1203−1208.
(59) Mezzetti, A.; Del Zotto, A.; Rigo, P.; Pahor, N. B. *J. Chem. Soc., Dalton Trans.* **1989**, 1045−1052.
(60) Smith, G.; Sutcliffe, L. H.; Cole-Hamilton, D. J. *J. Chem. Soc., Dalton Trans.* **1984**, 1209−1214.
(61) Smith, K.-T.; Rømming, C.; Tilset, M. *J. Am. Chem. Soc.* **1993**, *115*, 8681−8689.

important to report all temperature-dependent T_1 data as well as the T_1(min) value so that such effects can be detected.

The complexes **1Os** (X = Cl) and **2Os** (X = Br) are much more acidic than complex **5Os** (X = H). The trend in acidity as a function of ligand is mirrored by that of the hydride complexes $[OsH(C_5H_5)X(PPh_3)_2]^+$. This suggests that hydrogen−hydrogen bonding in these complexes with elongated dihydrogen ligands does not influence the acidity, except perhaps for **5Os**.

Acknowledgment. We are grateful to NSERC Canada and the donors of the Petroleum Research Fund as administered by the American Chemical Society for research grants and Johnson Matthey PLC for a loan of osmium salts. We thank Nick Plavac for some NMR results and Curt Koehler for technical assistance. The neutron diffraction study was carried out under Contract DE-AC02-76CH00016 with the U.S. DOE, Office of Basic Energy Sciences, Division of Chemical Sciences.

Supporting Information Available: Table of J(H,D) and T_1 values of 64 dihydrogen complexes, their classification as fast, intermediate, or slow spinning, and a plot showing this classification, and full details of the X-ray crystal structures of **1Os**PF_6 and **2Os**BF_4 and the neutron diffraction analysis of **1Os**PF_6 (49 pages). This material is contained in many libraries on microfiche, immediately follows this article in the microfilm version of this journal, can be ordered from the ACS, and can be downloaded from the Internet; see any current masthead page for ordering information and Internet access instructions.

JA9529044